

## Carbon-vacancy depth profile at the polar metastable $VC_{0.80}(111)-(1\times 1)$ surface studied by low-energy electron diffraction

J. Rundgren,\* Y. Gauthier, R. Baudoing-Savois, and Y. Joly

*Laboratoire de Spectrométrie Physique, Université Joseph Fourier, Boite Postale 87, F-38402 Saint-Martin d'Hères, France*

L. I. Johansson

*Department of Physics and Measurement Technology, Linköping University, S-58183 Linköping, Sweden*

(Received 8 July 1991)

The  $VC_{0.80}(111)$  surface forms a metastable  $1\times 1$  structure upon argon-ion bombardment and annealing at a temperature not exceeding 1000 K. We study this structure by low-energy electron diffraction and are able to determine the relaxation and composition of a four-layer slab inside the surface. The slab terminates with a vanadium layer at vacuum and is, to a good approximation, stoichiometric; the error bars of the carbon concentrations in layers two and four are estimated with great care. The interlayer spacing of the vanadium-carbon double layer next to vacuum is contracted 10% with respect to the (111) spacing of the bulk. We regard such a strong contraction, not observed on (111) surfaces of metals, as related to a compensating charge giving rise to a metastabilization of the polar (111) surface of vanadium carbide.

### I. INTRODUCTION

There is an extensive literature on the electronic properties of transition-metal carbides and nitrides of sodium-chloride structure.<sup>1</sup> These compounds generally contain vacancies in the nonmetal sublattice. Theoretical studies show<sup>2,3</sup> that vacancies give rise to new filled electron states located a few eV below the Fermi level. Particular features were actually observed around 2 eV below the Fermi level in photoemission spectra from polycrystalline TiN (Ref. 4), TiN(100) (Ref. 5), VN(100) (Ref. 6), VC(100) (Refs. 7 and 8), VC(110) (Ref. 9), polycrystalline ZrN (Ref. 4), ZrN(100) (Ref. 10), and polycrystalline NbC (Ref. 11), and were interpreted as originating from vacancy induced states. Theoretical calculations<sup>3</sup> indicate that a vacancy density gradient in the surface region will strongly affect the electronic structure and the photoemission spectra. Vacancy density gradients, created deliberately in the near-surface region by ion sputtering, and their modification upon annealing were investigated on (100) surfaces of TiC, TaC, and HfC by means of ion-scattering spectroscopy<sup>12</sup> and x-ray photoelectron spectroscopy.<sup>13</sup>

In the present low-energy-electron-diffraction (LEED) work, we study  $VC_{0.80}(111)$  in its  $1\times 1$  metastable state, and we find that a vacancy density gradient exists such that the crystal is terminated with a stoichiometric surface region. A distinct  $1\times 1$  LEED pattern is observed with an annealing temperature near 900 K, and a reconstructed three-domain  $1\times 8$  LEED pattern appears, when the annealing temperature is raised above 1000 K. The  $1\times 1$  structure is called metastable, since once obtained the  $1\times 8$  reconstruction lasts also in the low-temperature range. The (111) surface of vanadium carbide is polar. A polar surface is stabilized by a compensating charge<sup>14</sup> and in many cases this compensating charge is derived by a

reconstruction of the surface, including lattice rearrangement and segregation of vacancies.<sup>15</sup>

In a photoemission investigation of  $VC_{0.80}(111)$ , the surface reconstruction was found to affect the electronic structure with quite drastic changes,<sup>16</sup> whose origin could not be explained from electron energy bands calculated for the bulk lattice of  $VC_{1.0}$ . By means of transmission electron microscopy (TEM) on  $VC_x$  in the composition range  $x=0.75-0.86$ , a long-period superlattice was observed and interpreted as arising from carbon-vacancy ordering.<sup>17</sup> The superlattice was created above a critical temperature of about 1000 K but reversed to a disordered state at lower temperatures. TEM produced superlattice patterns on all three low-index surfaces,<sup>17</sup> while LEED shows a reconstructed pattern on the (111) surface<sup>16</sup> and nonreconstructed patterns on the (100) (Ref. 7) and (110) surfaces.<sup>9</sup>

The paper is organized as follows. Section II describes the preparation of a metastable  $1\times 1$  surface on  $VC_{0.80}(111)$  and the recording of LEED data. Section III lays out the elements of the LEED theory: first, the calculation of ion-core electron-scattering phase shifts by the linear muffin-tin orbital (LMTO) method; second, the application of the averaged  $t$ -matrix approximation (ATA) for modeling the scattering by carbon sites that contain some percentage of vacancies; and third, the characteristics of the computer program to be utilized for dynamical LEED calculations. Our structure model for  $VC_{0.80}(111)-(1\times 1)$  contains seven parameters pertaining to the lattice reconstruction, to the segregation of carbon site vacancies, and, inevitably, to the refractive inner potential. We discuss at some length how to fix the values of the nonstructural parameters with a purpose to secure a stable LEED optimization. In Sec. IV the structural analysis is carried out. We use both an automatic fit procedure with seven parameters and a grid search with six

parameters. The latter offers a possibility to estimate the uncertainty of the obtained surface parameters. Section V discusses the results and Sec. VI concludes the LEED study.

## II. EXPERIMENT

### A. Metastable $VC_{0.80}(111)-(1\times 1)$

Vanadium carbide has sodium-chloride structure. In the [111] direction, pure vanadium layers alternate with pure carbon layers. After a period of six layers, both the composition and the lateral displacements of the (111) layers are repeated, as illustrated in Fig. 1. Substoichiometric vanadium carbide has a complex phase diagram. With carbon atomic fractions 0.6–0.9, several structures of short-range or long-range order exist.<sup>18</sup> For instance, ordered  $V_6C_5$  and  $V_8C_7$  occur with carbon atomic fractions 0.73 and 0.88, respectively. The  $VC_{0.80}$  sample studied in the present work showed nothing but the sodium chloride structure in an investigation with x rays. It was spark cut from a rod grown by means of a vertical floating-zone technique,<sup>19</sup> and the chemical composition was determined by chemical analysis.<sup>20</sup>

The sample, a crystal slice about 12 mm in diameter and mounted on a goniometric head, was mechanically polished initially with paper and finally with diamond powder (down to 1- $\mu$ m grains). The residual misalignment between the polished surface and the crystallographic planes was found to be less than 0.1° from a comparison of laser beam reflections and x-ray reflections. The sample was then installed in a LEED goniometer equipped with a hemispherical glass screen and grids. The same optics were used for Auger electron spectroscopy (AES) in the retarding field mode to control the sample cleanliness. The polar angle of incidence and the azimuth of the crystal were set with a precision of 0.1°, and the residual crystal tilt was reduced to 0.1°. This accuracy, together with a good cancellation of magnetic fields, allowed us to obtain, to an excellent approximation, the same  $I$ - $V$  spectra for symmetrically equivalent beams. The base pressure was kept in the low  $10^{-10}$  Torr range, and a titanium trap cooled at liquid-nitrogen temperature reduced the partial pressure of contaminants.

After introduction in the chamber, the  $VC_{0.80}(111)$  sample was flash annealed at about 1500 K in order to recrystallize the surface perturbed by the polishing. A clean and reproducible surface was then routinely obtained by argon-ion bombardment followed by annealing. Heat treatment at 770–1000 K gives rise to a  $1\times 1$  LEED pattern reciprocal to the (111) layers of sodium-chloride type  $VC_{0.80}$ . Annealing above 1000 K gives rise to a reconstructed surface, visible as a superposition of  $1\times 8$  patterns, corresponding to three domains rotated 120° with respect to one another. On subsequent annealing in the lower-temperature regime, the threefold  $1\times 8$  pattern lasts. The  $1\times 1$  structure is characterized as metastable, because it is removed by the  $1\times 8$  structure in the manner just described. A necessary condition for the creation of a surface giving rise to a  $1\times 1$  pattern is that the low-temperature annealing is preceded by a strong argon-ion bombardment.

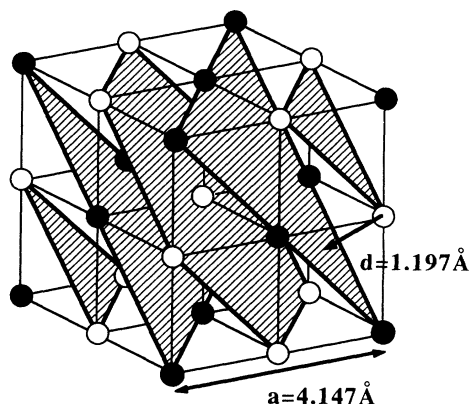


FIG. 1. The conventional unit cell of  $VC_{0.80}$ , which has sodium-chloride structure. With reference to the [111] direction, the crystal consists of periods of six layers with alternating atomic compositions, VCVCVC.

Under the heat treatment, the crystal underwent considerable strains that led to fractures, possibly due to a phase transition, and a large rhombic grain ( $\sim 5$ -mm side) developed in the middle of the sample. Its boundaries were marked and visible to the eye. The large grain was used in all our LEED and AES measurements of the  $1\times 1$  and  $1\times 8$  structures. In the present paper we focus our attention on the  $1\times 1$  metastable phase.

### B. LEED preliminaries

We expect that carbon segregates under the thermal treatment of the sample, so that the surface region has another structure than the bulk. The LEED experiment indicates that the outermost layers of  $VC_{0.80}(111)-(1\times 1)$  are substitutionally disordered. Any long-range or short-range ordering would have been visible as a complex LEED pattern or as streaks or poorly defined features in the elastic background. As concerns the geometrical arrangement of the (111) layers of the sodium-chloride structure, the layers are conventionally stacked in the  $ABC\dots$  sequence typical of a fcc crystal. But we are going to consider stacking faults parallel to the surface, since a carbon segregation could change the lateral registry of the layers near the surface. We investigate the cases where the terminal layer can be vanadium or carbon or, perhaps, a mixture of vanadium, carbon, and vacancies, and we consider a multiple relaxation of four interlayer spacings inside the surface.

The lattice parameter of vanadium carbide increases with the carbon content. It is 4.147 Å for  $VC_{0.80}$  (Ref. 21) and 4.182 Å for stoichiometric VC (Ref. 22), so that stoichiometric VC has a 1% greater lattice parameter than  $VC_{0.80}$ . In a previous LEED work we found that the surface region of  $VN_{0.89}(100)$  was approximately stoichiometric.<sup>23</sup> If, similarly,  $VC_{0.80}(111)-(1\times 1)$  is terminated by a stoichiometric surface slab that remains in registry with the bulk, we expect that the interlayer spacing is greater at the surface than in the bulk (with possibly the exception of the first spacing).

The intensity spectra were recorded in the range

30–280 eV in steps of 1 eV by means of a spot photometer mounted on a two-circle goniometer installed above a fluorescent screen.<sup>24</sup> We recorded (a) seven spectra at normal incidence and (b) nine spectra at oblique incidence, with the primary beam leaning 45° with respect to the surface normal and lying in the mirror plane through the surface normal and the  $[11\bar{2}]$  direction. The total energy ranges of the two sets of spectra were 1125 and 1950 eV, respectively. A 45° incidence was chosen with the purpose of increasing the LEED response to an expected gradient in the carbon-vacancy density near the surface. Before the LEED calculations, the diffuse background is subtracted, and the intensities are normalized to constant incident current.

### III. THEORY

#### A. Phase shifts

A calculation of the surface structure of  $\text{VC}_{0.80}(111)-(1 \times 1)$  comprises structural parameters, some of which give a strong LEED response, like an interlayer spacing close to the surface, and some of which give a comparatively weak response, like the carbon-vacancy density of a surface layer. Until now, it has not been known which sensitivity LEED has with respect to a vacancy density, and it is important to avoid as much as possible the competition of such a parameter with other structural and nonstructural parameters. In this work we attempt to calculate the electron-scattering phase shifts with no adjustable parameters other than a shift of the refractive inner potential.

The phase shifts for the ion cores of vanadium and carbon are calculated from a crystal potential obtained by the superposition of atomic electron densities. The superposition procedure starts from the same basic assumptions as the LMTO method.<sup>25</sup> The Wigner-Seitz spheres of vanadium and carbon in vanadium carbide fill up the volume of the unit cell and contain electron charges that make the unit cell neutral. A self-consistent LMTO band-structure calculation indicates a charge transfer of 0.10 electrons from carbon to vanadium.<sup>26</sup> In the superposition method, the charge transfer can be modeled by a renormalization of the overlap of the atomic electron densities. Madelung shifts<sup>25</sup> are included with the ion-core potentials, and muffin-tin radii are determined by the point where the potentials intersect on the line between the centers of the two ion cores. Vanadium and carbon then get muffin-tin radii 1.15 and 0.94 Å, respectively. The superposition potential gives an excellent approximation to the self-consistent LMTO band-structure potential referred to<sup>26</sup> and is found to be insensitive to small adjustments of the Wigner-Seitz radii and the charge transfer.

The superposition potential is a ground-state potential appropriate at primary energies near the Fermi level. However, in the energy range of LEED, the exchange-correlation part of the electron-scattering potential varies by several eV. We approximate the excited-state potential applying the Hedin-Lundqvist local-density method, as described in detail in an earlier LEED work.<sup>27</sup> The

electron-scattering phase shifts obtained from the excited-state potential are combined with an energy-dependent refractive inner potential. In the case of vanadium carbide, the latter is to a good approximation given by the following expression (in eV):

$$V_R = -3.5 - 88(E + 10)^{1/2}, \quad (1)$$

where  $V_R$  and the primary energy  $E$  are referred to the vacuum level. For example, when  $E$  is 60, 150, and 300 eV,  $V_R$  takes the values  $-14.0$ ,  $-10.5$ , and  $-8.5$  eV, respectively.

The expression for  $V_R$  depends on a particular crystal parameter that is unknown at the beginning of the LEED study, namely, the muffin-tin zero of the ground-state potential with respect to the vacuum level. Test calculations show that, if this parameter is shifted by a few eV,  $V_R$  is shifted together with an insignificant change of shape. We can thus establish an approximate value for the muffin-tin zero by preliminary LEED studies on  $\text{VC}_{0.80}(111)-(1 \times 1)$  and later improve the muffin-tin theory simply by shifting the inner potential in the course of the LEED optimizations. The absorptive part of the inner potential due to electron-gas attenuation is modeled by a phenomenological function of the primary energy (in eV),  $V_I = -0.85E^{1/3}$ .

The thermal vibrations of the crystal are accounted for by temperature-dependent phase shifts. Grimvall and Rundgren<sup>28</sup> propose a theory for determining the Debye temperatures of the species in the transition-metal carbides and nitrides of sodium-chloride type. Such a solid has the remarkably property that the two species vibrate with the same mean-square amplitude at high temperature. It turns out that the atomic Debye temperatures can be derived from the entropy of the solid when the relationship between entropy and mean-square amplitude is known for *one* crystal in the aforementioned category of solids. Referring to mean-square amplitudes measured for TiC and NbN by neutron-diffraction and helium-channeling experiments,<sup>29</sup> the theory gives calculated values for the Debye temperatures in  $\text{VN}_{0.89}(100)$  in excellent agreement with a LEED measurement.<sup>23</sup> By applying the same theory to vanadium carbide, we find the atomic Debye temperatures  $\Theta_D^V = 519$  K and  $\Theta_D^C = 1070$  K. An exploratory LEED study including the optimization of several surface parameters shows that these Debye temperatures can be used to a good approximation for all layers of  $\text{VC}_{0.80}(111)-(1 \times 1)$ .

#### B. Carbon-site vacancies and ATA

The electron scattering in a random binary compound can be described by ATA (Ref. 30). In cases where the binary compound segregates in a layerwise fashion, we consider a generalized ATA (Ref. 31), in which the layers contain atoms  $A$  and  $B$  with atomic fractions  $x_A^{(n)}$  and  $1 - x_A^{(n)}$  depending on the layer number  $n$ . The scattering amplitudes of randomized atom in layer  $n$  is then a linear combination of the scattering amplitudes  $t_{l,A}$  of atom  $A$  and  $t_{l,B}$  of atom  $B$ ,

$$t_{l,\text{alloy}}^{(n)} = x_A^{(n)} t_{l,A} + (1 - x_A^{(n)}) t_{l,B}, \quad (2)$$

where  $l$  labels the partial waves.

The validity of ATA for LEED from random alloys was recently corroborated by LEED calculations on the (100) surface of Pt-Ni alloys,<sup>32</sup> where ATA was compared with the coherent-potential approximation. Earlier ATA and LEED were successfully used for measuring the surface segregation on platinum-nickel alloys<sup>31,33-35</sup> and on platinum-iron alloys.<sup>33,36</sup> The combined methods reach an equally good agreement between theory and experiment as LEED on pure metals. The fact that the surface compositions found in this manner agree with the compositions obtained by AES,<sup>37</sup> x-ray photoemission spectroscopy,<sup>38</sup> and ion-scattering spectroscopy<sup>39</sup> is an empirical verification of the ATA-LEED procedure.

In the present work on VC<sub>0.80</sub>(111)-(1×1), each layer contains *a priori* one single species, vanadium or carbon. We consider the vanadium layers to be fully occupied and the carbon layers to have a vacancy density that varies with depth inside the surface. We model the electron scattering in the carbon layers by applying the ATA formula above with  $A$  replaced by carbon and  $B$  by a zero scatter. The effective scattering amplitudes of a mixture of carbon and vacancies are then approximated by the carbon atomic fraction  $x_C^{(n)}$  times the carbon scattering amplitude  $t_{l,C}$ . Previously, vacancies were studied by the application of ATA-LEED on Pt<sub>0.5</sub>Ni<sub>0.5</sub>(110) (Ref. 34), on Ru(100) with adsorbed hydrogen,<sup>40</sup> and on VN<sub>0.89</sub>(100) (Ref. 23).

Exploratory LEED calculations on VC<sub>0.80</sub>(111)-(1×1) indicate that the crystal terminates with a vanadium layer, and that layers with a random mixture of vanadium and carbon do not occur. Carbon thus occupies the layers 2,4,6,... We introduce the carbon atomic fractions  $c_2 = x_C^{(2)}$  and  $c_4 = x_C^{(4)}$  as variable parameters and fix the carbon atomic fraction of deeper layers at the bulk value 0.80, assuming that the LEED backscattering from layers below the fourth is too weak to resolve vacancy densities in individual layers. Estimating the error bars of  $c_2$  and  $c_4$  is a principal problem in this investigation.

### C. LEED program

The LEED program of Moritz<sup>41</sup> is utilized for calculating the  $I$ - $V$  spectra. It is a Korringa-Kohn-Rostoker (KKR) program equipped with different options for calculating the electron scattering by a stack of layers. One option uses matrix inversion for the intralayer scattering together with the plane-wave layer-doubling method for the interlayer scattering, and another option applies the partial-wave combined-space method. When the first option is used with a small interlayer spacing and heavy atoms in the layers, spurious effects can occur due to non-converging plane waves. The interlayer spacing is about 1.2 Å in VC<sub>0.80</sub>(111)-(1×1). Although vanadium and carbon are relatively weak scatterers, we carefully check that the layer-doubling method converges by applying both options of the program.

The above LEED program is included in an automatic fit procedure<sup>42</sup> designed to determine structural parameters from a given set of experimental spectra  $I_g^{\text{ex}}(V_i)$ , where  $g$  labels beams and  $i$  marks the points of the energy

grid. The procedure is a combination of a steepest-descent method and an expansion method, in which the theoretical spectra  $I_g^{\text{th}}(V_i)$  are considered as analytical functions of the surface parameters. The misfit between the theoretical and the experimental spectra is measured by an  $R$  factor called  $R_{\text{DE}}$  (DE for discrete energies): the sums over  $i$  of  $I_g^{\text{th}}(V_i)$  and  $I_g^{\text{ex}}(V_i)$  are normalized to unity for each beam  $g$ , and  $R_{\text{DE}}$  sums up the absolute differences  $I_g^{\text{th}}(V_i) - I_g^{\text{ex}}(V_i)$  over  $i$  and  $g$  in such a fashion that each  $g$  contribution is weighted by its particular number of energy points. The steepest-descent method gives rapid advance far from the optimum and the expansion method gives numerical stability near the optimum. The fit procedure is capable of determining the optimum in a multidimensional parameter space, where computing time would prohibit a search over grids. The optimization is stable with large energy steps, up to about 15 eV. In the next section we apply the fit procedure to seven parameters using 10-eV energy steps and the grid search to six parameters using 4-eV energy steps.

## IV. STRUCTURAL ANALYSIS

### A. Fit procedure

The fit procedure<sup>42</sup> is applied to a parameter space comprising four interlayer spacings  $d_1, d_2, d_3$ , and  $d_4$  from the surface and inwards, the carbon concentrations of layers two and four,  $c_2$  and  $c_4$ , and the shift of the refractive inner potential  $\Delta V_R$ . In addition, some other nonstructural parameters are varied during an early stage of the investigation, like the atomic Debye temperatures and the constants of the analytical expression for the refractive inner potential. But their values are fixed, as described in Sec. III A.

The fit procedure gives its lowest  $R_{\text{DE}}$  value with a surface model composed of layers stacked in the fcc fashion and terminated with a vanadium layer at vacuum. The optimum geometry and composition are given in Table I. The fit procedure referred to applies to spectra recorded at one single incidence. For seven spectra recorded at normal incidence, we obtain  $R_{\text{DE}} = 0.178$ , and for nine spectra recorded at 45° incidence  $R_{\text{DE}} = 0.273$ . The latter fit gives parameters whose values agree closely with the former, more sensitive fit. The result is illustrated in Fig. 2 by a side view cut perpendicularly through the surface.

The validity of the above results is controlled by particular runs of the fit procedure, as described below. Geometry and composition are varied separately and together over wide parameter intervals. In this manner we check that the obtained surface structure is a true optimum and not a subsidiary one.

The top layer consists of pure vanadium. This is the unambiguous result of fits starting from a composition initially set to a mixture of vanadium and carbon.

The surface layers have fcc stacking. To see this, we consider stacking faults in two layers inside the surface. In addition to the fcc stacking  $BCABC\dots$ , where the left-hand  $BC$  represents two surface layers and the subsequent  $ABC\dots$  the bulk, three other stackings are possible, namely  $ACABC\dots$ ,  $ABABC\dots$ , and

TABLE I. Surface parameters of  $VC_{0.80}(111)-(1 \times 1)$  from fit procedure: four interlayer spacings  $d_1$ ,  $d_2$ ,  $d_3$ , and  $d_4$  from vacuum and inwards, and carbon concentrations  $c_2$  and  $c_4$  in layers two and four:  $\Delta V_R$  is the shift of the inner potential.  $R_{DE}$  is the discrete-energy  $R$  factor. The last line gives the result when three spacings instead of four are considered, to be compared with the result of the grid search (see the lines “ $D_1$ ” and “Average” of Table II).

Incidence	$R_{DE}$	$d_1$ (Å)	$d_2$ (Å)	$d_3$ (Å)	$d_4$ (Å)	$c_2$ (at. %)	$c_4$ (at. %)	$\Delta V_R$ (eV)
0°	0.178	1.075	1.213	1.221	1.217	100	100	-2.28
45°	0.273	1.080	1.209	1.206	1.233	100	100	-2.32
Average		1.08	1.21	1.21	1.22	100	100	-2.3
Average		1.08	1.21	1.24		100	100	-1.7

$CBABC \dots$ . It turns out that the fcc stacking gives  $R_{DE}=0.178$  at normal incidence, whereas the stacking faults give  $R_{DE}=0.70, 0.65,$  and  $0.75,$  respectively. The possibility of stacking faults is therefore ruled out.

The spacings between (111) layers are  $1.197 \text{ \AA}$  and  $VC_{0.80}$  and  $1.207 \text{ \AA}$  in stoichiometric VC. The fact that we obtain  $d_2, d_3,$  and  $d_4$  values close to  $1.21 \text{ \AA}$  could indicate that the sample is stoichiometric from layer two and onwards in the surface region probed by LEED. We investigate this situation by applying the fit procedure to one surface model, where the surface net and the interlayer spacings  $d_n$  ( $n \geq 5$ ) correspond to the lattice constant of  $VC_{1.0}$ , and to another surface model, where the surface net corresponds to the lattice constant of  $VC_{0.80}$  and the interlayer spacings  $d_n$  ( $n \geq 5$ ) correspond to the lattice constant of  $VC_{0.10}$ . These models give  $R_{DE}=0.196$  and  $0.191,$  respectively, at normal incidence instead of the best  $R_{DE}$  value  $0.178$  mentioned above. We therefore conclude that the surface layers of  $VC_{0.80}(111)-(1 \times 1)$  are in registry with the bulk of  $VC_{0.80}$ .

The fit procedure is in fact sensitive to the carbon concentration. Tests made with alternatively 100 and 80 at. % in all carbon layers give  $R_{DE}=0.205$  and  $0.240,$  respectively, at normal incidence.

The fit procedure favors a refractive inner potential that is energy dependent.  $V_R$  defined by expression (1) and  $V_R$  assumed constant give  $R_{DE}=0.178$  and  $0.205,$  respectively, at normal incidence. The improvement of the

fit due to an excited-state electron-scattering potential is thus significant.

### B. Grid search

A grid search of structural parameters for finding an optimum surface model has two straight advantages. Spectra recorded at different incidence angles can be utilized simultaneously for optimizing parameters, and several metric distances (or  $R$  factors) can be applied so as to produce estimates of the error bars of the parameters.

We carry out a grid search in the six-dimensional space spanned by  $d_1, d_2, d_3, c_2, c_4,$  and  $\Delta V_R,$  considering 16  $I-V$  spectra recorded at normal and  $45^\circ$  incidence. To save computing time, we put  $d_4$  equal to the interlayer spacing in the bulk, knowing that the fit procedure shows a weak correlation between  $d_4$  and the other parameters. Suitable grids are extended over intervals containing the optimum values found by the fit, and the calculated and measured  $I-V$  spectra are compared by means of five metric distances: the strong metric distance  $D_1,$  the weak integrated metric distances  $D_2$  and  $D_{2y},$  and the Hausdorff metric distances  $D_4$  and  $D_{4y}.$  These metric distances are, in fact, all of the “discrete-energy” type and can be used with energy grids of any step length. In particular,  $R_{DE}=2D_1.$  The metric distances are described in detail in Ref. 43. The surface parameters versus metric distance obtained by the grid search are listed in Table II. The averaged result is virtually the same as with the fit procedure, and one finds that the value  $2D_1=0.24$  from Table II is roughly equal to the average of  $R_{DE}$  in Table I. The agreement between theory and experiment can be inspected on the  $I-V$  curves shown in Fig. 3.

When discussing the accuracy of the result, we follow a procedure utilized in two earlier LEED works.<sup>23,34</sup> In general, the standard deviation obtained from the averaging of a particular structural parameter over a set of metric distances can be used for estimating the uncertainty of the parameter value. However, under special circumstances, the standard deviation comes out zero. Such a case is presented by the carbon concentrations  $c_2$  and  $c_4,$  which take optimum values equal or very close to the physical cutoff 100 at. %. In all those cases in Table II where  $c_2$  or  $c_4$  attain the cutoff value, the gradient of the metric distance with respect to concentration turns out to

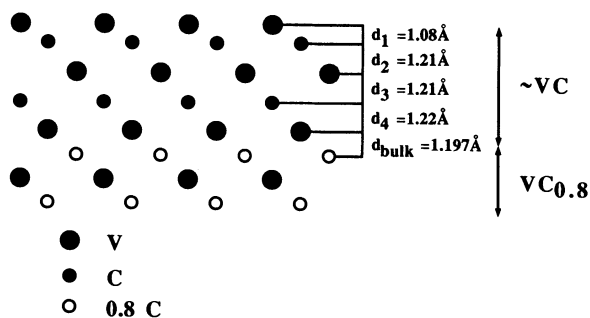


FIG. 2. Side view of the  $VC_{0.80}(111)-(1 \times 1)$  surface, projected on a plane through the surface normal and the  $[11\bar{2}]$  direction.

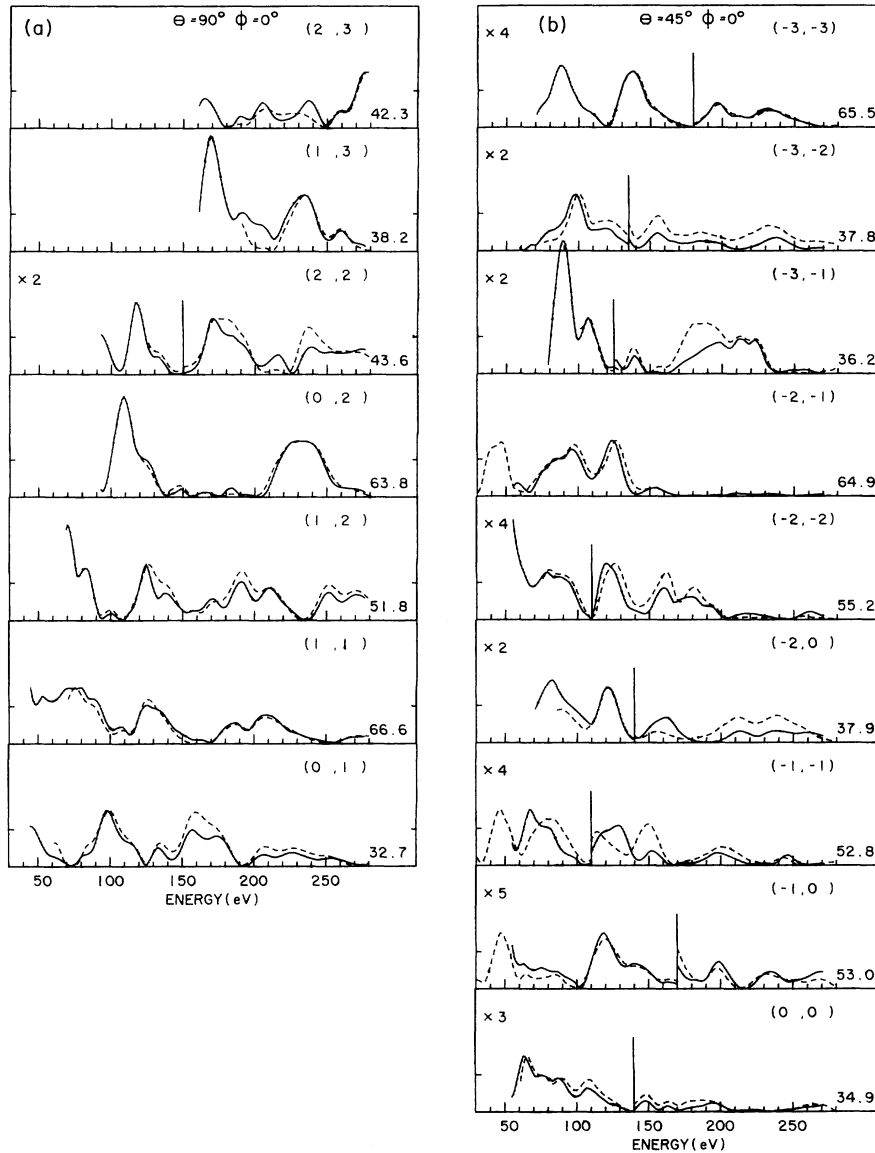


FIG. 3. The optimum surface model of  $VC_{0.80}(111)-(1 \times 1)$  is illustrated by theoretical (solid line) and experimental (dashed line)  $I$ - $V$  spectra. Values to the right of the curves: integrated experimental intensity divided by integrated theoretical density (the same units in all panels). (a) is incidence  $0^\circ$ , and (b) incidence  $45^\circ$  from the surface normal.

be negative finite. Of course, several optimizations giving exactly the same value produce no standard deviation.

Uncertainties can also be estimated from the concept of tolerance. We assume that a metric distance  $D$  can be determined with a tolerance  $D_{\min} - 1.01D_{\min}$ ; in other words, with a tolerance of 1%. Considering that the metric distance  $D$  has approximately a parabolic dependence on the parameters in the vicinity of  $D_{\min}$ , we calculate the variation  $\Delta p$  of each parameter  $p$  with all companion parameters kept constant, when  $D$  varies from  $D_{\min}$  to  $1.01D_{\min}$ . The parameter tolerances  $\Delta p$  obtained in this manner are given in Table II.

Standard deviations and tolerances can be combined by a maximum principle in such a fashion that they determine appropriate uncertainties for the whole set of parameters. The tolerance of  $D$  is adjusted to such a value that every parameter gets a tolerance  $\Delta p$  that is greater

than or equal to its standard deviation. This  $\Delta p$  will be referred to as the uncertainty of the parameter. The maximum principle is fulfilled by the parameters  $d_1$ ,  $d_2$ ,  $d_3$ , and  $\Delta V_R$ , provided the metric tolerance is adjusted to 1.4%. This metric tolerance is then used for assigning uncertainties to the carbon concentrations  $c_2$  and  $c_4$  (see Table II and Fig. 4). It turns out that the tolerance 1.4% follows from the standard deviation of the shift  $\Delta V_R$ , which thus determines the uncertainties of all the parameters in the case under consideration.

The uncertainties in the interlayer spacings and the carbon concentrations increase with increasing depth in the crystal due to the finite penetration of the LEED electrons. The vacancy density of the first carbon layer is found to be  $0_{-4}^{+0}$  at. % and that of the second carbon layer  $2_{-17}^{+2}$  at. %. These densities are significantly different from the vacancy density in the bulk, 20 at. %, and we

TABLE II. Surface parameters of  $VC_{0.80}(111)-(1 \times 1)$  obtained from grid search with two incidences  $0^\circ$  and  $45^\circ$ : three interlayer spacings  $d_1$ ,  $d_2$ , and  $d_3$  from vacuum and inwards, and carbon concentrations  $c_2$  and  $c_4$  in layers two and four;  $\Delta V_R$  is the shift of the inner potential. Metric distances between spectra: strong integrated distance  $D_1$ , weak integrated distances  $D_2$  and  $D_{2y}$ , and Hausdorff distances  $D_4$  and  $D_{4y}$ .

Metric (%)	$d_1^a$ (Å)	$d_2^b$ (Å)	$d_3^b$ (Å)	$c_2^c$ (at. %)	$c_4^c$ (at. %)	$\Delta V_R^d$ (eV)
$D_1 = 12.11$	1.074	1.213	1.240	100	92	-1.9
$D_2 = 3.32$	1.077	1.199	1.230	100	100	-3.1
$D_{2y} = 2.34$	1.078	1.199	1.228	100	100	-3.1
$D_4 = 6.57$	1.077	1.201	1.244	100	100	-4.4
$D_{4y} = 4.09$	1.077	1.200	1.237	100	100	-4.0
Average	1.07 <sub>6</sub>	1.20 <sub>2</sub>	1.23 <sub>6</sub>	100	98	-3.3
Standard deviation	0.001	0.006	0.006	0	3	1.0
Tolerance <sup>e</sup>	0.006	0.007	0.016	+0/-3	+2/-13	0.7
Uncertainty	0.01	0.01	0.02	+0/-4	+2/-17	1.0

<sup>a</sup>Grid  $d_1$  takes values from 1.037 to 1.137 Å in steps of 0.02 Å.

<sup>b</sup>Grids  $d_2$  and  $d_3$  take values from 1.177 to 1.257 Å in steps of 0.02 Å.

<sup>c</sup>Grids  $c_2$  and  $c_4 = 80, 90,$  and  $100$  at. %.

<sup>d</sup>Grid  $\Delta V_R$  takes values from -4 to 2 eV in steps of 1 eV.

<sup>e</sup>Corresponds to a tolerance  $D_{\min} - 1.01D_{\min}$  in the metric distances  $D$ .

conclude that the LEED optimization is able to determine surface parameters through a depth of four layers.

The determination of the refractive inner potential  $V_R$  deserves a comment. The fit procedure gives, at primary energies equal to 60, 150, and 300 eV, the values  $V_R = -16.3, -12.8,$  and  $-10.8$  eV, respectively, relative to a zero level in vacuum. The grid search gives, corre-

spondingly, the values  $V_R = -17.3, -13.8,$  and  $-11.8$  eV, with an uncertainty of  $\pm 1$  eV. At 60 eV primary energy, our  $V_R$  value corresponds approximately to the ground-state potential, but is found to be 1.3–2.3 eV lower than the band-structure value  $V_R = -15$  eV, calculated for  $VC_{1.0}$  (Ref. 44). We have found no other experi-

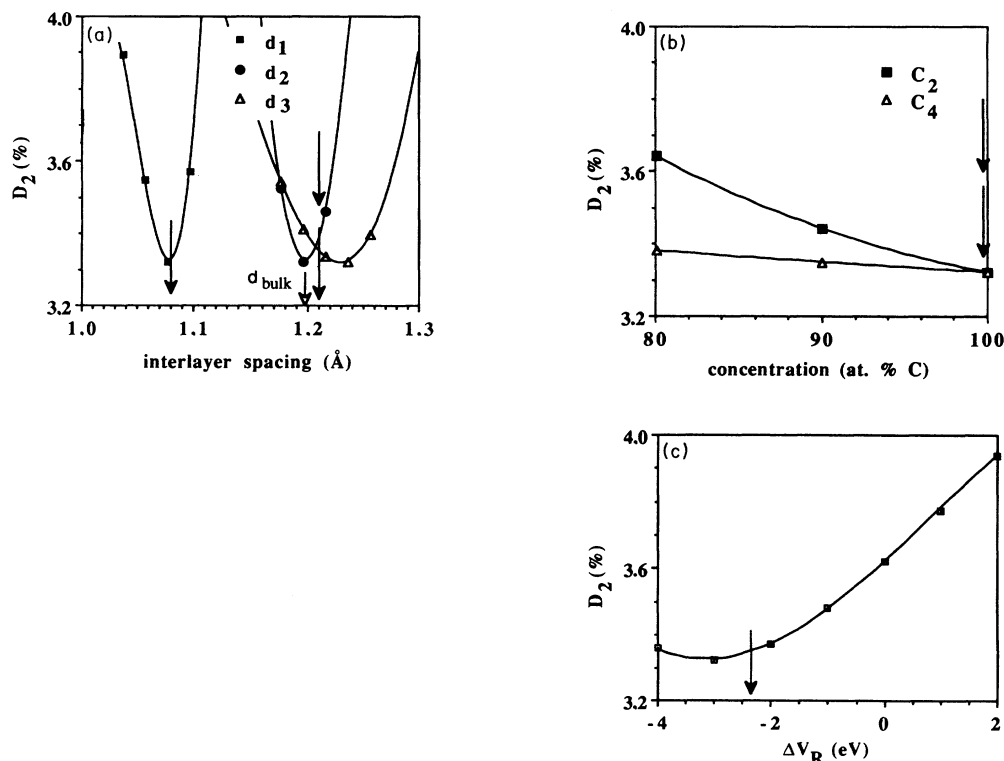


FIG. 4. The metric distance  $D_2$  illustrated as a function of (a) the interlayer spacings  $d_1$ ,  $d_2$ , and  $d_3$ , (b) the carbon concentrations  $c_2$  and  $c_4$  in the second and the fourth layers, and (c) the shift of refractive inner potential  $\Delta V_R$ . The arrows indicate the parameter values obtained by the fit procedure.

mental verification of the inner potential in vanadium carbide.

## V. RESULTS AND DISCUSSION

The surface structures obtained by the fit procedure listed in Table I and by the grid search listed in Table II agree within the estimated uncertainties of the parameters. In principle, the grid search should be more reliable, because it utilizes simultaneously the spectra recorded at normal and at oblique incidence, and it is based on as many as five misfit measures for comparing theoretical and experimental  $I$ - $V$  spectra. On the other hand, the fit procedure optimizes one parameter more,  $d_4$ , which we argue is resolvable from the given experimental data. When  $d_4$  is optimized, the optimum for  $d_3$  changes slightly from 1.23<sub>3</sub> and 1.22<sub>1</sub> Å, while the other distances remain virtually unchanged (the last two lines of Table I). In conclusion, owing to the remarkably good agreement between the two approaches when three spacings are considered, we take the outcome of the fit procedure with four spacings as the final result of this study.

LEED determines the structure of a four-layer slab of  $\text{VC}_{0.80}(111)-(1 \times 1)$ . The geometry and composition is  $d_1 = 1.08 \pm 0.01$  Å,  $d_2 = 1.21 \pm 0.01$  Å,  $d_3 = 1.21 \pm 0.02$  Å,  $c_2 = 100^{+0}_{-4}$  at. %, and  $c_4 = 98^{+2}_{-17}$  at. %. The fitted value for  $d_4$  is 1.22 Å, and the interlayer spacing in the bulk is 1.20 Å.

There is an excellent coherence among the surface parameters obtained by the fit procedure (separately at normal and oblique incidence) and by the grid search. The reliability of the LEED optimization is assessed by a low value of  $R_{\text{DE}}$  for the fit procedure (at normal incidence) and by low values of five metric distances for the grid search. The agreement between the theoretical and the experimental spectra is similar to what is obtainable on surfaces of clean metals or some bimetallic alloys.<sup>30,32-35</sup> The thickness of the surface slab probed by LEED with a significant layer-by-layer sensitivity is, in this case, about 5 Å. Concerning deeper layers with  $d_n$  ( $n > 5$ ) and  $c_n$  ( $n \geq 6$ ), LEED shows a sensitivity to average values of the parameters, as discussed in Sec. IV A.

The spacing between the layers of vanadium carbon at the top of  $\text{VC}_{0.80}(111)-(1 \times 1)$  is strongly contracted, by 10% with respect to the bulk spacing. Although  $\text{VC}_{0.80}(111)-(1 \times 1)$  is composed of hexagonal layers of vanadium and carbon stacked in the fcc fashion, it relaxes differently from fcc-type clean metals and random alloys, whose (111) surfaces are almost bulk terminated. We believe that the strong contraction is related to the stabilization of the polar surface by a compensating surface charge,<sup>14</sup> possibly achieved by a change of the charge transfer between vanadium and carbon in the bilayer next to the surface.

It is interesting to note that the interlayer spacings do not converge towards the bulk value within the four-layer slab, where LEED has a significant sensitivity to the surface parameters. The calculated composition profile corresponds to a stoichiometric surface compound  $\text{VC}_{1.0}$ . The two outermost carbon layers are enriched with carbon to such a degree that they contain no or almost no vacancies. The result that the interlayer spacings  $d_2$ ,  $d_3$ ,

and  $d_4$  are slightly larger than the spacing between the (111) layers of the bulk of  $\text{VC}_{0.80}$  is consistent with a picture where lateral strains are caused by the enrichment of carbon in the surface layers. The top layers remain in registry with the bulk, and a vertical expansion compensates for the strains within the layers.

Since four surface layers of  $\text{VC}_{0.80}(111)-(1 \times 1)$  are virtually stoichiometric, one would expect that valence-band photoemission spectra recorded from this surface could be explained by direct transitions between bulk bands calculated for  $\text{VC}_{1.0}$ . This is not the case, however,<sup>16</sup> and the reason may well be the strong contraction of the first vanadium-carbon interlayer spacing and an associated rearrangement of charges. The fact that no vacancy-related features were identified in previous photoemission spectra from  $\text{VC}_{0.80}(111)-(1 \times 1)$  is coherent with the LEED result that carbon-site vacancies begin to occur rather deep in the crystal, somewhere in layers 6, 8, . . . . Valence-band photoemission spectra recorded from the  $1 \times 8$  reconstructed surface of  $\text{VC}_{0.89}(111)$  showed spectral features that did not exist with the  $1 \times 1$  surface; a LEED study of the reconstructed surface will be reported elsewhere.

A vacancy density gradient at the surface of a transition-metal carbide or nitride of sodium-chloride type has now been established by LEED in two cases, namely with  $\text{VN}_{0.89}(100)$  (Ref. 23) and with  $\text{VC}_{0.80}(111)-(1 \times 1)$ . In the case of vanadium nitride, the surface layers are practically stoichiometric, containing half vanadium and half nitrogen with a density of nitrogen-site vacancies close to 0 at. %. The depth of the surface region where LEED indicates stoichiometry is not determined in Ref. 23, but we believe that it is of the order of 5 Å, as in the present investigation.

Transition-metal carbides can react differently on heat treatment. In the case of  $\text{VC}_{0.80}(111)$ , annealing temperature as low as 900 K produces a stoichiometric surface, and annealing above 100 K induces surface reconstruction. With the (100) surface of titanium carbide, argon ion bombardment and annealing at 1100 K give rise to a nonstoichiometric top layer containing  $10 \pm 2$  at. % vacancies, while heat treatment above 1300 K makes carbon segregate and fill up the vacancies.<sup>12</sup>

## VI. CONCLUSION

We conclude that LEED is able to determine relaxation and composition in a four-layer slab inside the surface of  $\text{VC}_{0.80}(111)-(1 \times 1)$ . The top layer is vanadium, and the carbon-site vacancy density has a gradient at the surface, so that the external four layers compose, to a good approximation, a stoichiometric slab. The interlayer spacing in the vanadium-carbon double layer next to the surface is contracted 10% with respect to the (111) spacing in the bulk. This is a much stronger relaxation than what is usually found with (111) surfaces of fcc metals.  $\text{VC}_{0.80}(111)-(1 \times 1)$  has a polar surface, and the strong contraction is possibly interconnected with a compensating surface charge making the surface metastable. The stable surface, reconstructed with threefold  $1 \times 8$  domains, will be pictured by scanning tunneling microscopy in a forthcoming paper.<sup>45</sup>



## ACKNOWLEDGMENTS

We are indebted to W. Moritz for providing the computer code used in the LEED calculations. Thanks are due to G. D'Assenza and C. Brun for technical assis-

tance during the preparation of the sample. Computing time was supplied by the Centre de Calcul Vectoriel pour la Recherche and by the National Supercomputer Centre in Sweden.

- \*Permanent address: Department of Theoretical Physics, Royal Institute of Technology, S-100 44 Stockholm, Sweden.
- <sup>1</sup>L. I. Johansson and C. G. Larsson, in *Angle Resolved Photoemission*, edited by S. D. Kevan (Springer, Berlin, 1991), Chap. 8, and references cited therein.
  - <sup>2</sup>P. Marksteiner, P. Weinberger, A. Neckel, R. Zeller, and P. H. Dedrichs, *Phys. Rev. B* **33**, 812 (1986); J. Redinger, *Solid State Commun.* **61**, 133 (1987).
  - <sup>3</sup>J. Redinger, P. Weinberger, and A. Neckel, *Phys. Rev. B* **35**, 5647 (1987); **35**, 5652 (1987).
  - <sup>4</sup>H. Höchst, R. D. Bringans, P. Steiner, and Th. Wolf, *Phys. Rev. B* **25**, 7183 (1982).
  - <sup>5</sup>P. A. P. Lindberg, L. I. Johansson, J. B. Lindström, and D. S. L. Law, *Phys. Rev. B* **36**, 939 (1987).
  - <sup>6</sup>J. B. Lindström, P. A. P. Lindberg, L. I. Johansson, D. S. L. Law, and A. N. Christensen, *Phys. Rev. B* **36**, 9514 (1987).
  - <sup>7</sup>P. A. P. Lindberg, L. I. Johansson, and A. N. Christensen, *Surf. Sci.* **192**, 353 (1987).
  - <sup>8</sup>P. A. P. Lindberg and L. I. Johansson, *Z. Phys. B* **68**, 83 (1988).
  - <sup>9</sup>L. A. P. Lindberg, L. I. Johansson, and A. N. Christensen, *Z. Phys. B* **69**, 521 (1988).
  - <sup>10</sup>J. B. Lindström, L. I. Johansson, A. Callenas, D. S. L. Law, and A. N. Christensen, *Phys. Rev. B* **35**, 7891 (1987).
  - <sup>11</sup>H. Höchst, P. Steiner, S. Hüfner, and C. Politis, *Z. Phys. B* **37**, 27 (1980).
  - <sup>12</sup>M. Aono, Y. Hou, R. Souda, C. Oshima, S. Otani, and Y. Ishizawa, *Phys. Rev. Lett.* **50**, 1293 (1983).
  - <sup>13</sup>G. R. Gruzalski and D. M. Zehner, *Phys. Rev. B* **42**, 2768 (1990).
  - <sup>14</sup>M. Tsukada and T. Hoshino, *J. Phys. Soc. Jpn.* **51**, 2562 (1982); W. Ebert and H. H. Kung, *Surf. Sci.* **155**, 313 (1985).
  - <sup>15</sup>S. Zaima, Y. Shibata, H. Adachi, C. Oshima, S. Otani, M. Aono, and Y. Ishizawa, *Surf. Sci.* **157**, 380 (1985).
  - <sup>16</sup>P. L. Wincott, P. A. P. Lindberg, and L. I. Johansson (unpublished).
  - <sup>17</sup>J. D. Venables, D. Kahn, and R. G. Lye, *Philos. Mag.* **18**, 177 (1968); J. Billingham, P. S. Bell, and M. H. Lewis, *ibid.* **25**, 661 (1972).
  - <sup>18</sup>J. P. Landesman, G. Treglia, P. Turchi, and F. Ducastelle, *J. Phys. (Paris) Colloq.* **46**, CX-1001 (1985), and references cited therein.
  - <sup>19</sup>A. N. Christensen, *J. Cryst. Growth* **33**, 99 (1976).
  - <sup>20</sup>The chemical analysis of the VC<sub>0.80</sub> sample was made at AB Sandvik Hard Materials, Box 42056, S-12612 Stockholm, Sweden.
  - <sup>21</sup>The lattice constant is 4.147 Å for VC<sub>0.80</sub> from linear interpolation between the lattice constants 4.131 Å for VC<sub>0.73</sub> and 4.166 Å for VC<sub>0.88</sub> (from experimental results on metal carbides and nitrides compiled by C. H. de Novion and published in Ref. [18]).
  - <sup>22</sup>A. Neckel, P. Rastl, R. Eibler, P. Weinberger, and K. Schwarz, *J. Phys. C* **9**, 579 (1976).
  - <sup>23</sup>Y. Gauthier, Y. Joly, J. Rundgren, L. I. Johansson, and P. Wincott, *Phys. Rev. B* **42**, 9328 (1990).
  - <sup>24</sup>L. de Bersuder, *Rev. Sci. Instrum.* **45**, 1569 (1974).
  - <sup>25</sup>H. L. Skriver, *The LMTO Method* (Springer, Berlin, 1984).
  - <sup>26</sup>J. Häglund, G. Grimvall, T. Jarlberg, and A. F. Guillet, *Phys. Rev. B* **44**, 2914 (1991).
  - <sup>27</sup>R. E. Watson, J. F. Herbst, L. Hodges, B. I. Lundqvist, and W. Wilkins, *Phys. Rev. B* **13**, 1463 (1976); J. Neve, J. Rundgren, and P. Westrin, *J. Phys. C* **15**, 4391 (1982); J. Neve, P. Westrin, and J. Rundgren, *ibid.* **16**, 1291 (1983).
  - <sup>28</sup>G. Grimvall and J. Rundgren (unpublished).
  - <sup>29</sup>R. Kauffman and O. Meyer, *Solid State Commun.* **51**, 539 (1984).
  - <sup>30</sup>B. L. Györfy and G. M. Stocks, in *Electrons in Disordered Metals and at Metallic Surfaces*, edited by P. Phariseau, B. L. Györfy, and L. Scheire (Plenum, New York, 1979).
  - <sup>31</sup>Y. Gauthier, Y. Joly, R. Baudoing, and J. Rundgren, *Phys. Rev. B* **31**, 6216 (1985).
  - <sup>32</sup>S. Crampin and P. J. Rous, *Surf. Sci.* **244**, L137 (1991).
  - <sup>33</sup>Y. Gauthier and R. Baudoing, in *Segregation and Related Phenomena*, edited by P. Dowben and A. Miller (CRC, Boca Raton, 1990).
  - <sup>34</sup>Y. Gauthier, R. Baudoing, M. Lundberg, and J. Rundgren, *Phys. Rev. B* **35**, 7867 (1987).
  - <sup>35</sup>R. Baudoing, Y. Gauthier, M. Lundberg, and J. Rundgren, *J. Phys. C* **19**, 2825 (1986); Y. Gauthier, R. Baudoing, and J. Jupille, *Phys. Rev. B* **40**, 1500 (1989); Y. Gauthier, W. Hoffmann, and M. Wüttig, *Surf. Sci.* **233**, 239 (1990).
  - <sup>36</sup>P. Beccat, Y. Gauthier, and R. Baudoing, *Surf. Sci.* **238**, 105 (1990).
  - <sup>37</sup>D. Dufayard, R. Baudoing, and Y. Gauthier, *Surf. Sci.* **233**, 223 (1990).
  - <sup>38</sup>Y. Jugnet, G. Grenet, N. S. Prakash, Tran Min Duc, and H. C. Poon, *Phys. Rev. B* **38**, 5281 (1988).
  - <sup>39</sup>L. de Temmerman, C. Creemers, H. Van Hove, A. Neyens, J. C. Bertolini, and J. Massardier, *Surf. Sci.* **178**, 888 (1986); S. Deckers, F. H. P. M. Habraken, W. F. van der Weg, A. W. Denier van der Gon, B. Pluis, J. F. van der Veen, and R. Baudoing, *Phys. Rev. B* **42**, 3253 (1990).
  - <sup>40</sup>M. Lindroos, H. Pfnür, and D. Menzel, *Surf. Sci.* **192**, 421 (1987).
  - <sup>41</sup>W. Moritz, *J. Phys. C* **17**, 353 (1984).
  - <sup>42</sup>G. Kleinle, W. Moritz, D. L. Adams, and G. Ertl, *Surf. Sci.* **219**, L637 (1989); G. Kleinle, W. Moritz, and G. Ertl, *ibid.* **238**, 119 (1990).
  - <sup>43</sup>J. Philip and J. Rundgren, in *Determination of Surface Structure by LEED*, edited by P. M. Marcus and F. Jona (Plenum, New York, 1984); S. A. Lindgren, L. Walldén, J. Rundgren, and P. Westrin, *Phys. Rev. B* **29**, 576 (1984).
  - <sup>44</sup>The Fermi energy is 10.5 eV from Ref. 22 and 10.3 eV from Ref. 26. The work function for VC(111) is not available, but we use the value 4.7 eV for TiC(111) (Ref. 15).
  - <sup>45</sup>M. Hammar, C. Törnevik, J. Rundgren, Y. Gauthier, A. Flodström, K. I. Hakansson, L. I. Johansson, and J. Häglund, *Phys. Rev. B* (to be published).